

Original Article

Development of a murine intravesical orthotopic human bladder cancer (mio-hBC) model

Peter A Raven¹, Ninadh M D'Costa¹, Igor Moskalev¹, Zheng Tan¹, Sebastian Frees^{1,2}, Claudia Chavez-Munoz¹, Alan I So¹

¹Vancouver Prostate Centre, Department of Urologic Sciences, University of British Columbia, Vancouver, BC, Canada; ²Universitätsmedizin der Johannes Gutenberg-Universität Mainz, Mainz, Germany

Received October 31, 2018; Accepted December 14, 2018; Epub December 20, 2018; Published December 30, 2018

Abstract: We have developed a murine intravesical orthotopic human bladder cancer (mio-hBC) model for the establishment of superficial urothelial cell carcinomas. In this model we catheterize female athymic nude mice and pre-treat the bladder with poly-L-lysine for 15 minutes, followed by intravesical instillation of luciferase-transfected human UM-UC-3 cells. Cancer cells are quantified by bioluminescent imaging which has been validated by small animal ultrasound. Poly-L-lysine pre-treatment increased engraftment rate (84.4%) and resulted in faster growing tumors than trypsin pre-treatment. In addition, tumors respond through a decrease in growth and increase in apoptosis to chemotherapy with mitomycin C. Previous intravesical models utilized KU7 cells which have been later determined to be of non-bladder origin. They display markers consistent with HeLa cells, requiring a need for a true intravesical bladder model. Efficient engraftment and rapid superficial growth patterning of the human bladder tumor differentiate this *in vivo* orthotopic model from previous bladder models.

Keywords: Intravesical, orthotopic, murine, xenograft, bladder cancer, human model, cell line

Introduction

In 2017, it is estimated that there will be 8,900 new cases of bladder cancer occurring in Canada and 2,400 Canadians will die from the disease [1]. Non-muscle invasive bladder cancer accounts for approximately 70% of all bladder cancer cases. The standard treatment for patients with non-invasive disease is transurethral resection with adjuvant intravesical treatments in select patients with high risk features. Even with optimal treatments, 60-70% of these tumors will recur, with 25% showing progression to a higher stage or grade highlighting a need to develop novel therapies [2].

In vitro assays using cultured primary or bladder cancer cell lines provide valuable data to study mechanism of development, mutagenesis, invasion, migration and evaluation of anti-neoplastic drugs. However, there are a number of limitations such as environmental differences, loss of natural heterogeneity, loss of vascularization and perfusion, artificial levels of

growth factors and cytokines within the cell culture media. Most importantly, *in vitro* cell culture is limited to 1 to 2 different types of cells in monolayer restricting the study of the interactions between cell types [3].

To overcome this, animal models are needed to facilitate the study of carcinogenesis mechanisms while avoiding the limitations of the *in vitro* studies. Thus, a suitable bladder tumor model that resembles human disease both histologically and in behavior is essential for evaluating new therapeutic agents and modalities. The ideal animal bladder tumor model should include the following characteristics: 1) Tumor should grow intravesically (orthotopically to allow for interaction with normal urothelium, lamina propria and muscle layers). 2) Tumor should be of urothelial carcinoma origin to mimic the natural history of bladder cancer progression. 3) Tumor should be technically easy to develop within a reasonable time period and highly reproducible and reliable.

Many different bladder cancer animal models have been developed and fall mainly into syngeneic, xenogeneic and transgenic categories. Syngeneic models include those developed with chemical carcinogens [4-7] or mouse tumor cells implanted into mice, sometimes orthotopically into the bladder [8-16]. These tumors generally have high engraftment rates but a disadvantage of mouse tumors is that microenvironmental interactions and molecular characteristics of the tumor cells must be confirmed to recapitulate human tumors, especially if an experimental therapeutic has a molecular target. Xenogeneic models utilize human cancer cells and can more closely resemble human tumors. These models can also mimic microenvironment effects if implanted orthotopically [17-21] rather than subcutaneously [22-28]. These models pose an additional challenge to engraftment from the murine host and often require a pre-treatment of the bladder. Genetically modified animal models provide a unique system in which the role of individual genes in bladder cancer development can be evaluated [29-33]. However, the models are either very toxic or extremely expensive, and no model has shown to provide a reliable molecular proxy for human carcinoma [32, 33].

Orthotopic xenografts have shown to be a better approach allowing cell-cell interactions of the local environment that more closely mimic superficial bladder cancer (non-muscle invasive) in which primary tumor grows in the urothelium and progresses to invasion into the muscle layers of the bladder [8, 34]. A previous and highly cited intravesical model developed by our group used KU7 cells with high reproducibility and engraftment rate without a pre-treatment of the bladder [18]. Unfortunately, we found that KU7 cells display HeLa genetic markers and as such do not mimic the bladder cancer environment [41]. Therefore, we have developed a murine intravesical orthotopic human bladder cancer (mio-hBC) model utilizing true human bladder cancer cells.

Materials and methods

Animals

Ninety eight 6-week old female athymic nu/nu mice were used to carry out this project (Envigo, South Kent, Washington, USA). All animal pro-

cedures were performed according to the guidelines of the Canadian Council on Animal Care (CCAC). The protocol was approved by the Animal Care Committee of the University of British Columbia (Protocol No. A15-0073). Animals were monitored daily and scored according to our clinical health monitoring sheet. Clinical signs that were considered severely abnormal were considered humane endpoints for this study such as, more than 20% body weight loss; attitude immobile or hyper reactive, even when nudged; appearance hunched, dry or dull eyes and nose, jaundice, pale extremities, ulceration on the tumor site; breathing gasping, cyanosis; posture tumor interferes with movement; hydration skin tent (>2 sec), sunken eyes, no urine output >12 h; elimination excessive or no urination, watery or bloody diarrhea, rectal prolapse that cannot be corrected; abdomen with severe distension; body conditions emaciated, no palpable fat pad over sacroiliac region, severely reduced muscle mass, prominent vertebrae and iliac crests. If the mouse had a score of 3 in any of the above mentioned categories or a cumulative score of 6 or higher it was euthanized. Also, tumor weight >10% (therapeutic) of normal body weight, or tumors exceeding a bioluminescence of 1×10^{10} photons/sec, pain that cannot be relieved by analgesia, or hematuria, or urethral obstruction, or ascites where burden exceeded 10% of body weight, or persistent self-induced trauma were also considered endpoints. Mice exhibiting the mentioned criteria were euthanized and removed from the study. Mouse numbers were determined by power analysis using an alpha of 0.05, beta of 0.8, predicted difference in tumor size of 3×10^6 photons/sec and predicted standard deviation of 1×10^6 photons/sec and determined by preliminary data.

Experimental design

This study was designed in 4 stages. The first stage consisted of evaluating our previous published protocol, that unfortunately was carried out with a cell line that at the time was considered to be a human bladder cancer cell line (KU7) but after published we found out it was from HeLa origin. Therefore, we decided to follow the same protocol but with a well-known non-muscle invasive bladder cancer cell line (UM-UC-3 cells). For this first stage we used 10 six-week old athymic female mice. Due to the results found in our first stage, we had to modi-

Murine model for bladder cancer

fy our previously published protocol. The modifications lead to the second stage of this study, which consisted of the evaluation of pre-treatments (trypsin and poly-L-lysine) and its tolerability. For this second stage we used 20 six-week old athymic female mice. Once finding out the most appropriate pre-treatment with less side effects, we moved into the third stage, which consisted of evaluating tumor engraftment using several human bladder cancer cell lines (UM-UC-3-luc, UM-UC-14-luc, TCC-Sup-luc, T24-luc, J82-luc, 5637-luc and RT-112-luc). For this third stage we used 52 six-week old athymic female mice. Our final fourth stage consisted of a functional assay (mitomycin C treatment), to test our optimized non-muscle invasive bladder cancer model. For this final fourth stage we used 16 six-week old athymic female mice.

Procedure

Mice were anesthetized using isoflurane at 3% for induction and then switched to 1.8% as maintenance at 2 L/min oxygen. Each mouse was placed on a heating pad and the bladder was manually emptied. Under continuous anesthesia and using aseptic surgical techniques a 25G catheter was inserted through the urethra. Poly-L-lysine, trypsin or PBS pre-treatments were applied to the bladder by instilling 50 μ L of 0.1% poly-L-lysine [35], 0.25% trypsin [36] (ThermoFisher Scientific, Burlington, ON, CA) or PBS (Sigma-Aldrich Canada Co., Oakville, Ontario, Canada) and letting it dwell for 15 min before removing the catheter [18] and emptying the bladder manually. Bladder cancer cells in suspension were intravesical instilled (luciferase transfected UM-UC-3-luc, UM-UC-14-luc, TCC-Sup-luc, T24-luc, J82-luc, 5637-luc and RT-112-luc) into the bladder at a density of 3×10^6 cells in 50 μ L. A Vasco-Statt plastic clamp (midi, angled) was placed around the urethral meatus to avoid leakage of the inoculated cells. The inoculated solution was kept in the bladder for 1.5 h through which the mice were kept under anesthesia. During this time, the mice were surveilled for changes in respiratory patterns, skin color and temperature. After 1.5 h the clamp and the catheter were removed and the bladder emptied spontaneously. At this moment the mice were removed from anesthesia and placed into a heated recovery chamber until they were mobile and urinating normally.

In-vivo functional assay utilizing mitomycin C

In order to demonstrate the use of our described model we treated tumors with mitomycin C post inoculation. Mitomycin C was chosen because of its clinical use as a neoadjuvant chemotherapy. Eight mice were assigned to each of a phosphate-buffered saline (PBS) and mitomycin C treatment group and treated at days 8 and 15 as described below and assessed up to day 23. Mice were instilled with saline (82.5 μ L) or mitomycin C (3.3 mg/kg in 82.5 μ L solution, Sigma-Aldrich Canada Co.) for 1.5 h following the protocol described for tumor inoculation.

Cell culture

Human bladder cancer cell lines UM-UC-3 (ATCC CRL-1749), UM-UC-14 (ECACC 080905-09), T24 (ATCC HTB-4), and TCC-Sup (ATCC HTB-5) were kindly provided by Dr. Peter Black (Vancouver Prostate Centre, Vancouver, BC, Canada) and J82 (ATCC HTB-1) and 5637 (ATCC HTB-9) and RT-112 (ECACC 85061106) were kindly provided by Dr. Yoshiyuki Matsui (Kyoto University, Kyoto, Japan). All cells were cultured at 37°C in a 5% CO₂ incubator in minimal essential medium (Thermo Fisher Scientific) supplemented with 10% fetal bovine serum (Hyclone, South Logan, Utah, USA) 1% L-glutamine (GlutaMax, Thermo Fisher Scientific), 1% non-essential amino acids (Thermo Fisher Scientific, Burlington, Ontario, Canada), and 1% sodium pyruvate (Thermo Fisher Scientific). Mycoplasma contamination was tested at regular intervals for each cell-line. Before being used for in vivo testing, cells were trypsinized (0.25% trypsin, Thermo Fisher Scientific), and centrifuged at 200 \times g for 5 min. Cell pellets were re-suspended in media, counted using a TC20 (Biorad, Hercules, California, USA), centrifuged and re-suspended in media at a concentration of 3×10^6 cells per 50 μ L. Cells were immediately placed on ice until instillation.

Luciferase transfection of bladder cancer cell lines

The firefly luciferase gene was transfected into each parental cell line to generate luciferase equivalents (e.g. UM-UC-3-luc) using lentiviral construct as previously described [18]. Briefly, a mixture of 10 μ g of FUGWB transducing vector, 10 μ g pRO.91 packaging vector and 5 μ g vesicular stomatitis virus glycoprotein (VSV-G)

Murine model for bladder cancer

encoding plasmid was added to 37 μ l of CaCl_2 (2 M, pH 7.2). 2X HEPES buffer was then added to the DNA-calcium complex and incubated for 30 min. After 30 min incubation, the complex solution was added to HEK 293T cells. The media of infected HEK 293T cells was changed after 24 h and after additional 24 h the media containing recombinant lentiviral vector was collected, filtered with 0.45 μ m filter and added to bladder cancer cell lines for transduction. The luciferase plasmids contained blasticidin resistance gene to enable positive selection with 10 mg/mL blasticidin (ThermoFisher Scientific). Quantitative PCR was performed to ensure transcription of luciferase and luciferase activity was tested by adding D-Luciferin (150 μ g/mL, GoldBio, St. Louis, Missouri, USA) before measuring bioluminescence on an IVIS Spectrum (Perkin Elmer, Waltham, Massachusetts, USA).

Tumor imaging

IVIS Bioluminescence: For all experiments animals were measured twice a week. At each imaging mice were anesthetized with isoflurane, weighed, and intraperitoneally injected with 15 mg/kg sterile D-luciferin in PBS. Fifteen minutes following injection mice were placed in a supine position in an IVIS Spectrum bioluminescent imager and photographed at 10 min post injection using Living Image 4.0 software. Data was collected as photons/second and displayed as a regionalized heat map with increasing intensity from blue to red.

Ultrasound: Imaging was performed once weekly on a Vevo 700 ultrasonic device from Visual Sonics (Toronto, Ontario, Canada) that consists of a high frequency scanhead (20-60 MHz) allowing a resolution of 30 microns. Mice were anesthetized and placed on a heating pad with body temperature and heart rate monitoring. In order to visualize the bladders they were distended by injecting 100 μ L of PBS via a 25G catheter which was left in place. Sterile ultrasound gel was applied to the skin overlying the bladder and the scan head was positioned on the abdominal wall. Images were captured by serial imaging every 5 mm throughout the entire bladder.

Tissue harvesting

At experiment end, mice were euthanized using 5% isoflurane anesthetization followed by cervi-

cal dislocation. Full bladders were excised and preserved by immersion in 10% formalin for 24 hour before being transferred to 70% ethanol until processed and embedded in paraffin.

Immunohistochemistry

Following formalin fixation, tissues were processed and embedded in paraffin. Sections (4 μ m) were then prepared and mounted on slides for staining. De-paraffinization was performed by incubating slides at 60°C for 1 hour followed by repeated xylene and ethanol submersion. Antigen retrieval was performed by immersing slides in a container of 0.1 M citrate buffer (pH 6.0) and steaming for 30 min after which they were rinsed with water and incubated with 3% hydrogen peroxide for 3 minutes and rinsed again. Blocking buffer (2.5% bovine serum albumin in PBS) was applied to the sections and allowed to incubate for 1 hour at room temperature.

Ki67 (MA5-14520, monoclonal rabbit, ThermoFisher Scientific) staining was performed by incubating slides over night at 4°C with the primary antibodies at 1:50 concentration in Dako Antibody Diluent (Agilent Technologies, Santa Clara, CA, USA). Slides were rinsed in PBS and incubated for 1 hour at room temperature in a secondary HRP conjugated antibody at 1:1000 concentration before being rinsed again. Terminal deoxynucleotidyl transferase nick end labelling (TUNEL) was performed by incubating slides for one hour at 37°C with terminal deoxynucleotidyl transferase enzyme in a buffered solution containing bromodeoxyuridine (BrdU) incorporated nucleotides, rinsing with PBS, and incubating with an anti-BrdU antibody conjugated to biotin before rinsing again. A secondary HRP conjugated antibody was applied as mentioned above. All slides above were stained with a DAB+ kit (Agilent Technologies) for 30 minutes, rinsed and stained with hematoxylin.

For H&E staining, slides were immersed for one minute in Mayer's hematoxylin solution (Sigma-Aldrich Canada Co., Oakville, ON, CA), rinsed for 15 minutes with water, exposed to reagent alcohol for 30 seconds, immersed in eosin Y solution (Sigma-Aldrich Canada Co.) for one minute and rinsed again. All slides were dehydrated by repeated submersion in ethanol and then xylene, and coverslips were affixed using Cytoseal XYL (Thermo Fisher Scientific). Images were captured on a Zeiss Axioplan upright

Murine model for bladder cancer

microscope and processed using Zen software suite (Zeiss, Oberkochen, Germany).

Statistical analysis

All data is represented by means +/- standard error. Tumor sizes were reported as raw detection of number of photons/sec. Differences between groups were determined by t-test or ANOVA and growth rates were determined by a t-test on slopes in SigmaPlot (Systat Software Inc., San Jose, California, USA). $P \leq 0.05$ was considered statistically significant. All experiments were repeated in triplicate and in three independent experiments.

Results

Luciferase transfected bladder cell lines showed linear luminescence with cell number

In order to quantify tumor size all bladder cancer cell lines (UM-UC-3, UM-UC-14, T24, TCC-Sup, J82, 5637 and RT-112) were permanently transfected with a luciferase gene construct by lentiviral transfection as previously described under material and methods. This allows cells to be detected by bioluminescent imaging through the abdominal wall [18]. All cells showed high emissions of photons (2.5×10^6 photons/sec from 1×10^4 cells). Furthermore, photon emission values measured *in vitro* are different from those measured *in vivo* due to interference by the abdominal wall in mice. Therefore, we optimized the number of cells required for efficient bioluminescent intensities before intravesical instillation. We found that luciferase expressing bladder cell lines luminesce linearly with cell number in UM-UC-3 (**Figure 1A**) and in the other transfected bladder cancer cell lines. Coefficients of determination varied from 0.95 to 0.99 depending on the cell line (data not shown) indicating that luminescence is a good proxy for cell number. Given the photon emission values *in vitro* and the expected interference of the mouse bladder and abdominal wall, we chose a cell number 10 fold greater (approximately 3×10^6) to ensure equivalent photon transmission in initial *in vivo* trials. A previous validation has shown similar results [19, 37].

Bladder tumors did not engraft using the previously published KU7 protocol

Once all bladder cancer cell lines were successfully expressing luciferase, we decided to

use the tumor instillation protocol from our previously published bladder cancer model. Unfortunately KU7 cells were previously considered a bladder cancer cell line and later demonstrated also by our group to show a HeLa cell genotype. We needed a certified human bladder cancer cell line so we selected UM-UC-3-luc cells, which is a human bladder cancer cell line of transitional cell carcinoma and of epithelial origin.

In a pilot study 10 athymic six-week old mice, were intravesically inoculated with UM-UC-3-luc cells (procedure mentioned under material and methods). Results showed only 2 mice out of 10 with successful tumor engraftment, demonstrating a very low engraftment rate when instilled using the previously published protocol for KU7 cells (**Figure 1B**). In comparison KU7 results from preliminary data during the initial model development show an engraftment rate of 90% (9 of 10 mice, **Figure 1C**). In addition, initial tumor sizes three days after instillation are much smaller in those 2 mice ($8.90 \times 10^4 \pm 3.72 \times 10^4$ photons/sec) than results shown in our previous model using KU7 ($2.92 \times 10^6 \pm 4.94 \times 10^5$ photons/sec; $P = 0.04$). We were evaluating pre-treatment options when we published the first model and it is evident that bladder cancer cells require a bladder pre-treatment to increase engraftment rate.

Poly-L-lysine pre-treatment is better tolerated than trypsin

Since our previous published model did not show an adequate engraftment when using certified bladder cancer cell lines, we decided to evaluate the use of pre-treatments before intravesically inoculating the bladder with human bladder cancer cell lines. Animal models for intravesical engraftment have used trypsin to open the junctions between the epithelial cells and remove the umbrella layer cells in the bladder lumen [36]. This presumably allows for a better attachment site. Poly-L-lysine has also been used as a pre-treatment reagent in a previously published bladder cancer syngeneic model [35]. Poly-L-lysine coats the lumen with a positive charge and aids in tumor cell adhesion. In this study, we evaluated the use of trypsin and poly-L lysine as pre-treatments to further achieve tumor engraftment. Bladder pre-treatment with 0.25% trypsin for 15 minutes resulted in gross hematuria in 60% (6 of 10)

Murine model for bladder cancer

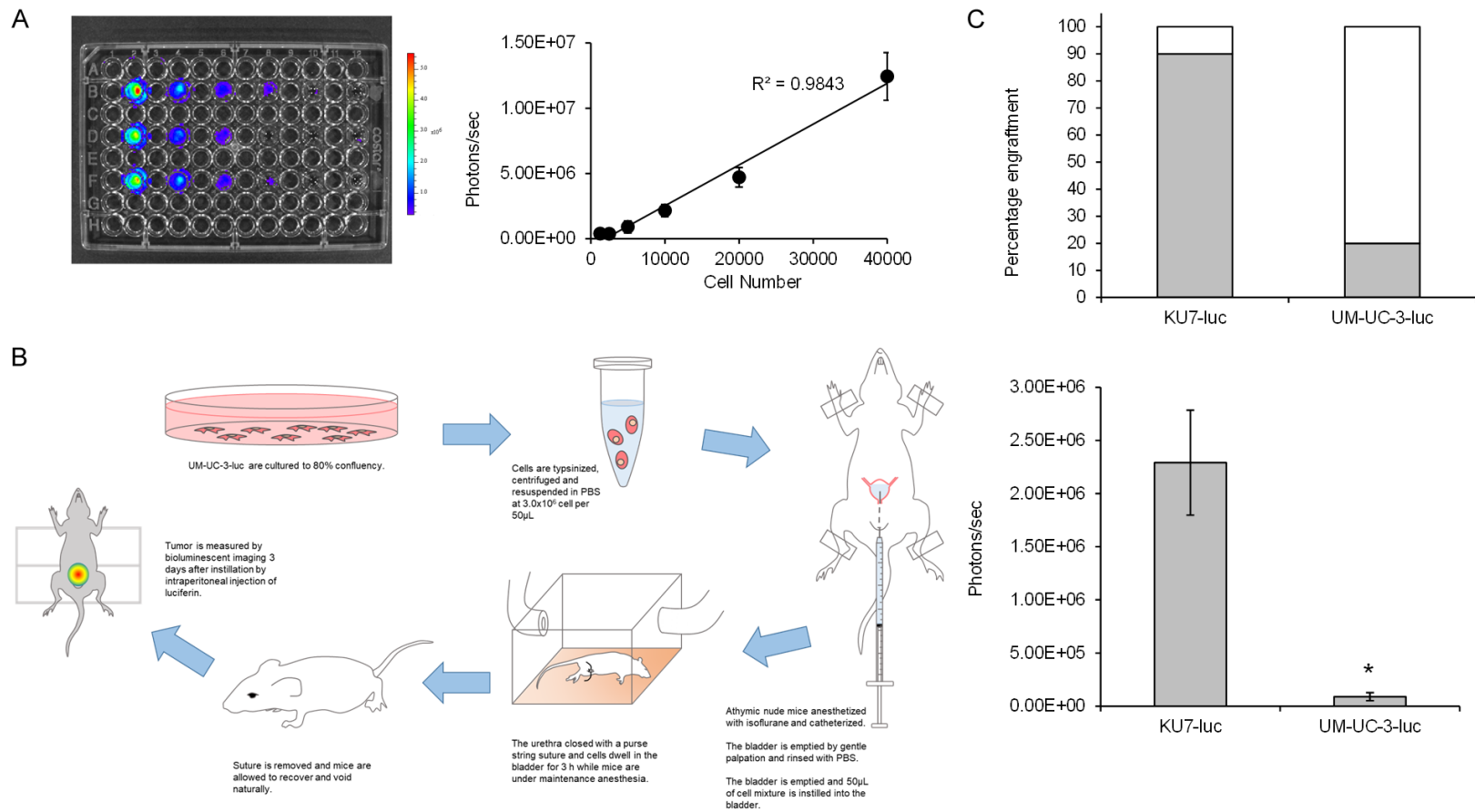


Figure 1. Protocol used to instill KU7 cells is not effective for bladder cancer cells. A. Bladder cancer cells bioluminesce linearly with cell number as seen, for example, in UM-UC-3-luc cells. B. Schematic of the protocol used to instill KU7-luc cells. C. Engraftment percentages and initial tumor size of KU7-luc and UM-UC-3-luc tumors using this protocol. Asterisks denote significant differences. $P \leq 0.05$, $N = 10$.

Murine model for bladder cancer

Table 1. Pre-treatment tolerance

Clinical Presentation	Pre-treatment	
	0.25% Trypsin	0.1% Poly-L-lysine
Total mice treated	10	10
Hunching	4	1
Scratching	0	0
>20% Weight loss	0	0
Hematuria	6	0
Other behaviour changes	3	0
Mice unaffected	4	9

of mice and as a result these mice reached humane endpoint within the first day (**Table 1**). In addition, these mice presented with hunching and other abnormal behaviors such as lethargy and shaking. Four of ten mice were unaffected by trypsin pre-treatment. Bladder pre-treatment with 0.1% poly-L lysine showed no adverse clinical signs in 90% of the animals tested (9 out of 10). Only one mouse treated with poly-L-lysine presented with hunching, which was observed for one day without needing to exclude the animal from the study. We could not determine whether the hunching was due to the pre-treatment, catheterization or anesthesia. Given the low rate of side effects from poly-L-lysine, we chose this pre-treatment when evaluating bladder cancer cell engraftment rates.

UM-UC-3 engraft and grow in a modified instillation procedure

In order to achieve successful engraftment rates, the previously published bladder cancer model had to be modified and optimized. Furthermore, this procedure was used to evaluate a wide variety of different bladder cancer cell lines as shown in **Figure 2A** and **2B**.

Procedural modifications included (**Figure 2A**): 1. Resuspension of cells prior to implantation in growth media rather than PBS in order to prevent cells from becoming nutrient limited over the length of the instillation procedure. 2. Pre-treatment of the bladder for 15 minutes with 0.1% Poly-L-lysine. 3. Substitution of the purse string suture with a Vascu-Stat plastic clamp (midi, angled) to reduce urethral injury. 4. Decrease in the dwell time of the cancer cells from 3 h to 1.5 h to reduce urine reflux. Our earlier model [18] utilized a 3 h dwell time but our preliminary data found that when using

UM-UC-3 cells up to 46.7% of mice (10 of 21) can develop kidney tumors due to urine reflux. We did not optimize all dwell times but found that halving the time to 1.5 h lowered the rate of kidney tumors to 3.9%.

Bladder cancer cell lines showed high variability in initial engraftment rate in which some tumors failed to engraft as defined by a background level of luminescence (UM-UC-14-luc, 7 of 7; TCC-Sup-luc, 0 of 7, T24-luc, 4 of 7; J82-luc, 6 of 7; 5637, 6 of 7; RT-112 0 of 7; **Figure 2B**). UM-UC-14-luc and J82-luc did not grow over a 30-day period. 5637-luc showed very modest growth (3.9 ± 0.49 fold) but did not grow to a suitable extent to test therapeutics (**Figure 2B**). Conversely, T24-luc grew well at 24.7 ± 0.49 fold (P = 0.070, N = 7) over a two-month period, but due to the low bioluminescence immediately after instillation ($7.52 \times 10^4 \pm 1.35 \times 10^4$ photons/sec) tumor size at experiment end did not surpass even the initial sizes of either UM-UC-14-luc ($2.54 \times 10^6 \pm 6.30 \times 10^5$ photons/sec) or 5637-luc ($3.65 \times 10^6 \pm 1.19 \times 10^6$ photons/sec) tumors. UM-UC-3-luc tumors grew quickly and reached a final size approximately 2100 fold larger than initial instillation over 30 days ($3.27 \times 10^9 \pm 1.98 \times 10^9$ photons/sec; P = 0.05 N = 10). In addition to increased growth, UM-UC-3-luc tumors appeared to be less variable in initial size than other bladder cancer cell lines. An example of tumor variability in UM-UC-14-luc and UM-UC-3-luc is shown in **Figure 2B**.

Tumor gross appearance by ultrasound corroborates bioluminescent activity

To compare the actual tumor size and measured luminescence, we have used ultrasound technology to visualize tumor growth. Comparative views of a selected tumor's growth via bioluminescent imaging and small animal ultrasound can be seen in **Figure 3A** and **3B**. A region of interest was marked on the mouse at initial imaging and bioluminescence can be reliably compared over time using standardized software instrument settings (**Figure 3A**). A single tumor can be measured as it grows and the bioluminescence level compared to the number of cells that was determined *in vitro*. In addition, bioluminescence can be corroborated by ultrasound imaging of tumors *in vivo* as shown for a select mouse in **Figure 3B**. Our

Murine model for bladder cancer

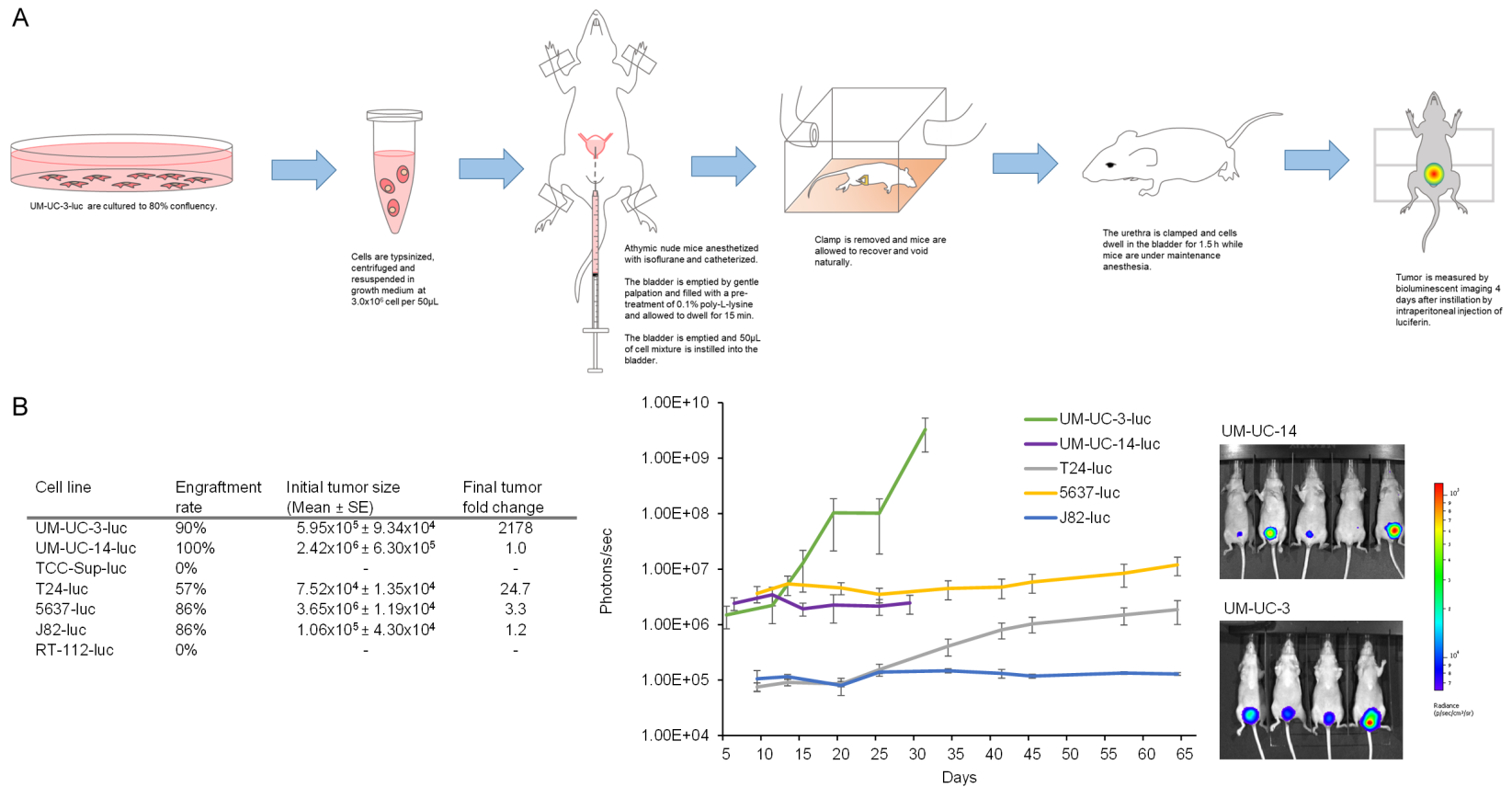


Figure 2. UM-UC-3-luc cells engraft and grow quickly with poly-L-lysine pre-treatment and a modified instillation protocol. A. The modified instillation protocol to instill UM-UC-3-luc tumors. B. Engraftment and growth (as measured by bioluminescence) of bladder cancer cells instilled using the new protocol and an example of reduced variability in initial tumor sizes of UM-UC-3-luc tumors relative to other cell lines. N = 7-10.

Murine model for bladder cancer

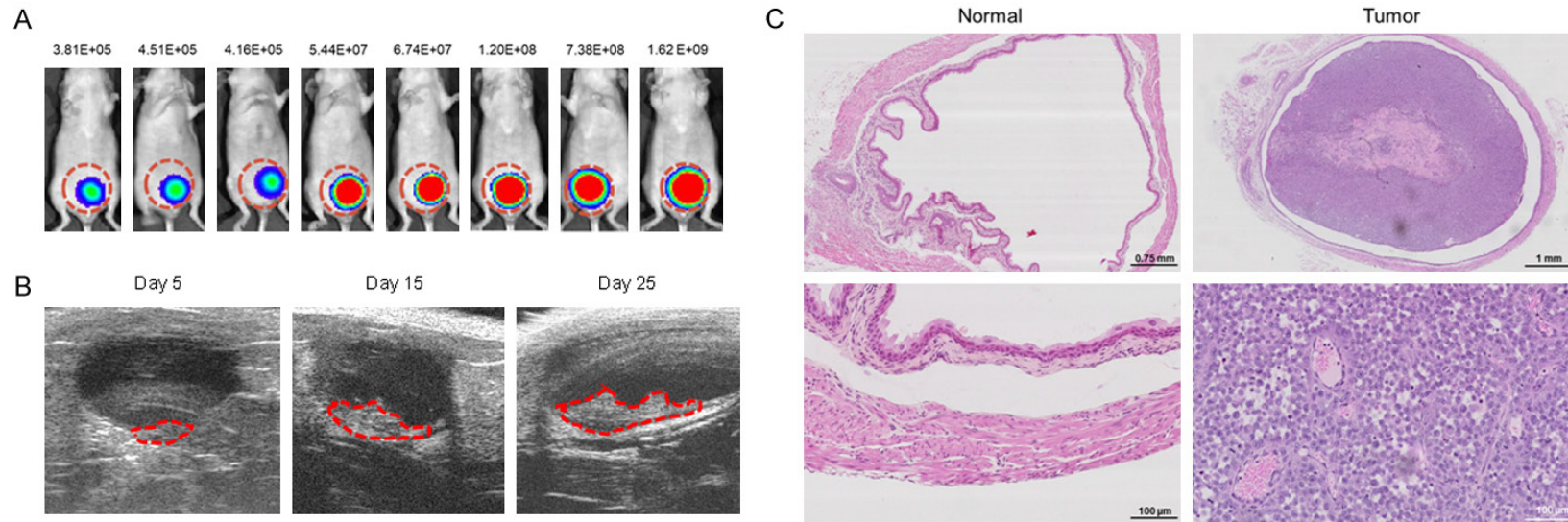


Figure 3. Growth in UM-UC-3-luc tumors visualized by bioluminescent imaging, small animal ultrasound and immunohistochemistry. A. Images of a select mouse showing bioluminescence over the course of the experiment. Luminescence values are given above the images. The orange circle delineated the region of interest for measuring tumor luminescence. B. Select ultrasound images of the bladder with tumors outlined in red at days 5, 15 and 25. C. Hematoxylin and eosin (H&E) staining of normal mouse bladder and a bladder containing a UM-UC-3-luc tumor. Image of the entire normal bladder and enlarged image of the urothelium show normal stratified cells layers. The bladder containing a tumor is much larger with a stretched urothelium. The centre of the tumor is highly necrotic. The enlarged image of the tumor in a non-necrotic region shows vascularization and a lack of normal tissue patterning.

results substantiate that luminescence intensity is linearly correlated with tumor size ($R^2 = 0.97 \pm 0.02$, $N = 5$, data not shown) as has been previously determined [37].

This bladder tumor model mimics patient tumors

Primary tumors in the urothelium are vascularized and have cell-cell interaction with the local environment. To establish that our bladder cancer tumors in this model have similar microenvironment, we have taken sections of the tumor for histological analysis. Histology of a large UM-UC-3-luc tumor shows dense cell growth with large nuclei and prominent nucleoli (**Figure 3C**). Some vascularization has occurred but the tumor is vastly necrotic in the centre due to insufficient blood supply and oxygenation. We were also able to observe that if UM-UC-3-luc tumors were left to grow longer, tumors were able to fill the bladder causing urethral obstruction which was considered an absolute endpoint in our model. One mouse out of 46 during our experimentation showed this and is represented in **Figure 3C** (histological sections).

In order to determine that the UM-UC-3-luc tumors recapitulate a patient tumor we performed a functional assay and treated established tumors with a chemotherapeutic, mitomycin C, as would occur in a clinical setting (**Figure 4A**). This treatment was applied when tumors were small in the 1×10^6 photons/sec range. Tumor size was significantly different starting at day 12. At day 21, control PBS treated tumors were 107 fold larger than mitomycin C treated tumors (PBS, $4.19 \times 10^7 \pm 1.58 \times 10^7$ photons/sec; mitomycin C, $3.88 \times 10^5 \pm 1.57 \times 10^5$ photons/sec; $P = 0.01$, $N = 8$). At day 21 the mitomycin C treated tumors were not significantly different in size to the beginning of the trial at day 4 (day 21, $3.88 \times 10^5 \pm 1.57 \times 10^5$ photons/sec; day 4, $1.61 \times 10^5 \pm 3.70 \times 10^4$ photons/sec; $P = 0.65$; $N = 8$) but the PBS control tumors had increased to 200 fold their starting size (day 21, $4.19 \times 10^7 \pm 1.58 \times 10^7$ photons/sec; day 4, $2.09 \times 10^5 \pm 9.66 \times 10^4$; $P = 0.01$; $N = 8$). This reduction in tumor growth suggests a complete response to mitomycin C treatment. Slope analysis to compare growth rates show that the control group grew significantly faster over the experiment (control slope, 0.09 ± 0.03 ; mitomycin C slope, -0.03 ± 0.02 ; $P = 0.007$, $N = 8$).

Immunohistological staining of the treated tumors with H&E, Ki67 as a marker for proliferation and Tunel as a marker for apoptosis, shows that the surface of the tumor has been affected by mitomycin C treatment (**Figure 4B**). Diffuse proliferation (more than 10% of tumor cells) and apoptosis can also be seen throughout the tumor. Untreated tumors (PBS control) show a staining pattern similar to what was observed in **Figure 4**. We can conclude that this model is responsive to conventional therapy and will be a suitable model for experimental therapeutics.

We have found no evidence of tumor invasion in our sections at experiment end. UM-UC-3 is a basal-type, transitional cell carcinoma cell line of epithelial origin with mutations in p53 and Kras and a mesenchymal, poorly-differentiated phenotype [38]. The tumors may have the potential, given enough time, to invade but further study is required to determine if this is possible. Eventual tumor invasion would be consistent with many non-muscle invasive bladder cancers (NMIBC) that further progress to muscle invasive bladder cancers (MIBC).

Discussion

A wide variety of bladder cancer animal models have been previously utilized to evaluate experimental treatments and these have highlighted common pitfalls in model development. Firstly, it is technically more challenging to establish an orthotopic model in the bladder than to establish tumors subcutaneously. The proper placement within the bladder is also a challenge as the natural history of urothelial carcinoma involves transition from a luminal superficial tumor to an aggressive muscle invasive tumor. The appropriate stage must be chosen in advance. Secondly, tumor take rate can vary greatly depending on tumor cell inoculation location, and the choice of chemical or physical pre-treatment methods to increase engraftment rate. Thirdly, tumor establishment can be time consuming and unreliable. Initial tumors may grow quickly and spread beyond the intended site or too slowly to be practical for drug screening or treatment trials. Lastly, tumors may initially engraft in off target sites, potentially impeding physiological function and being unsuitable for the intended trial.

Mouse models for *in vivo* studies of bladder cancer have been in use for decades and fall

Murine model for bladder cancer

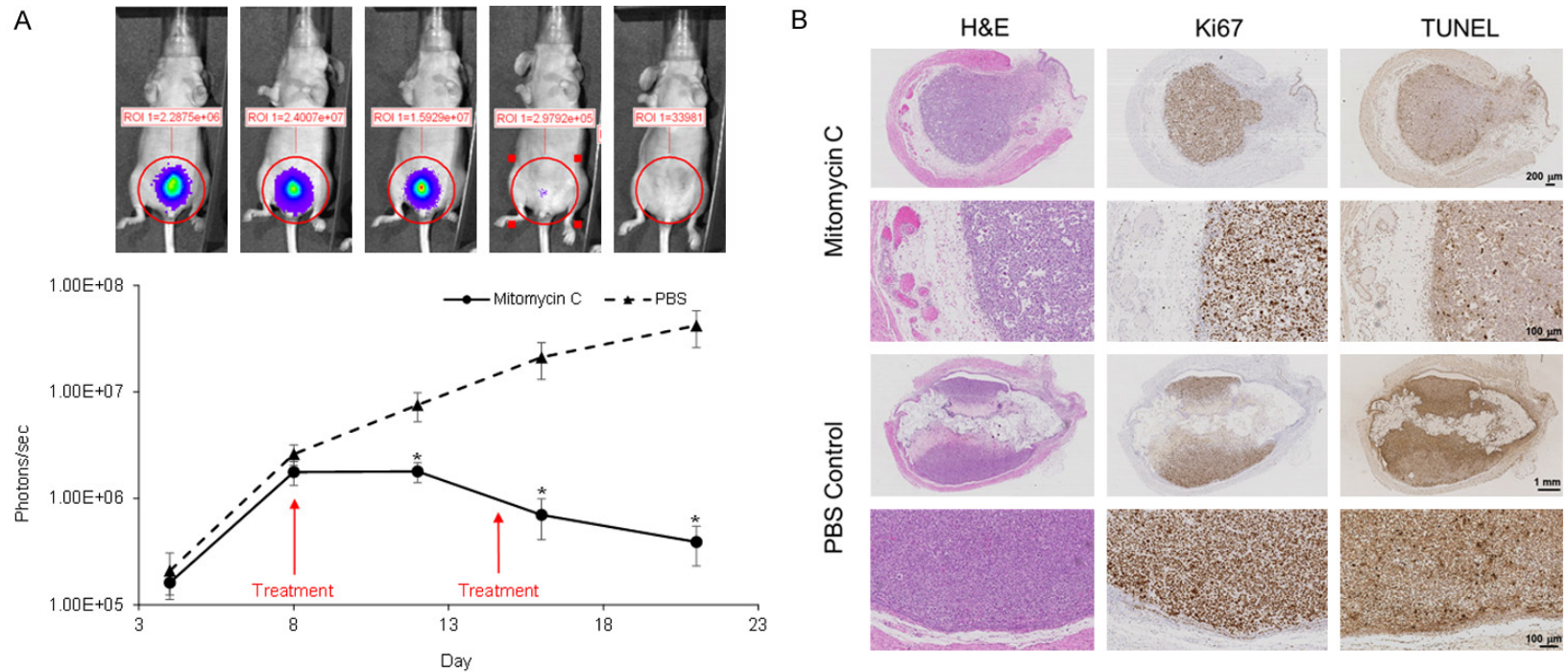


Figure 4. UM-UC-3-luc tumors respond to intravesical mitomycin C. A. Following treatment with 3.3 mg/kg mitomycin C tumor growth is arrested and then reduced compared to saline control (PBS). B. Hematoxylin and eosin (H&E) staining of a mitomycin C treated tumor. Ki67 shows cell proliferation in the centre of the mitomycin C treated tumor but not the edge exposed to the drug. Control tumors are proliferating in the non-necrotic areas. TUNEL shows apoptosis in the outer edge of the mitomycin C treated tumor where it was in contact with the drug and less so in the tumor centre. On the other hand, TUNEL is strongly present in the necrotic centre of control tumors. Asterisk denotes significant difference. $P \leq 0.05$, $N = 8$.

Murine model for bladder cancer

mainly into three categories: syngeneic models, xenograft models and transgenic models. Syngeneic models include those in which bladder cancer develops *in situ*, orthotopic models of mouse cell lines implanted into the mouse bladder and implantation outside the cell-originating site, most commonly subcutaneously. A major disadvantage of all syngeneic models is that they require the use of mouse-derived tumors. Results obtained from these models can only be applied to human carcinoma if it is first determined that the mouse microenvironment and tumor cells are physiologically and biochemically similar to what is seen in patients. For these reasons the use of a human-derived bladder cancer cell line (UM-UC-3 in our model) is often preferred. An important characteristic of syngeneic models is the intact immune system of the host mouse. Mouse bladder cancer cells can effectively evade the adapted immune response of the host mouse and will often engraft and grow. This is ideal for studies requiring an immune component.

In situ syngeneic bladder tumors can be initiated with chemical carcinogens such as the nitrosamines N-Nitrosodimethylamine (NMDA) and N-butyl-N-(4-hydroxybutyl) nitrosamine (BBN) introduced in drinking water [7, 39] or through exposure of the bladder lumen to the parasite haemotobium [7]. Similar tumors arise in some patients with exposure to these agents making this model suitable for those carcinomas but many patients develop transitional cell carcinoma without toxic exposure and its associated mutagenic effects. In such cases, these models may not be applicable. Furthermore, a significant amount of time is needed to develop tumors in these models (commonly on the order of months) which may be unsuitable for large trials. It can therefore be advantageous to have a treatable tumor within a week of orthotopic instillation.

Early syngeneic orthotopic models have been extensively reviewed by Chan et al. (1999) and have been modified since [9-11, 13-16, 29, 37, 40]. The strength of an orthotopic model is that the developing tumor will experience a micro environment similar to the natural tumor state and can interact with the appropriate tumor associated cells. Unfortunately, these models still operate under the restriction of all syngeneic models and assume that the mouse cells recapitulate the human counterparts. In addition,

tumor take rates can be variable in these models, requiring more mice than the tumors required. A variety of techniques to enhance take rate have been employed and will be discussed below.

Non-orthotopic syngeneic models are commonly used due to the ease of establishing the tumor, the high take rate (often 100%) and the speed at which they grow. Sub-cutaneous injection of MBT-2 tumor cells in the flank and/or shoulder of C3H/He mice is one such example [12]. If treatments are to be applied intravenously or by intra-tumoral injection, then this model will suffice despite the lack of a proper microenvironment. An assumption must be made that the stromal compartment of the skin epithelium sufficiently recapitulates that of the bladder if results from these models are applied to bladder cancers. Orthotopic trials are necessary to remove these potentially confounding factors. Despite this caveat, exploratory trials of new therapeutics can be reliably tested in this model before moving into an orthotopic trial.

Unlike syngeneic models, xenograft models allow for *in vivo* studies using human bladder cancer cell lines that have been validated *in vitro* to be similar to a human tumor. The adapted immune response of the host mice used in syngeneic models leads to rejection of human xenografts and results in a very low take rate. Thus, mice with a compromised adapted immune response such as athymic nu/nu mice or compromised adapted and native immune responses such as severe combined immunodeficiency (SCID) mice are best used. As a result, xenograft models are unsuitable for cancer immunity studies. Orthotopic [17, 18, 20, 21, 41] and non-orthotopic [22-28, 42] xenograft models are both used with disadvantages and benefits similar to orthotopic and non-orthotopic syngeneic models.

The third group of mouse bladder models includes the varieties of transgenic mice with spontaneous bladder carcinoma development [30, 31]. Each genetic alteration can be used to model mutations seen in existing bladder cancer patients without the complexity of tumor implantation. The drawbacks are the high cost of transgenic mice and the specificity of the genetic alteration. The tumors do not represent the comprehensive changes seen in a bladder

Murine model for bladder cancer

tumor from a human patient or cell line resulting from cellular adaptation throughout the life of the tumor.

Our model addresses many of the shortcomings of existing models and our previous model utilizing KU7 cells. We have established an orthotopic xenograft model utilizing fast growing UM-UC-3 cells in athymic nude mice. As such, tumors are human cell line derived unlike syngeneic models and experience the natural tumor microenvironment of the bladder absent in non-orthotopic models. Additionally, tumors develop within a week unlike BBN-induced or spontaneous *in situ* models and the use of athymic nude mice is cost effective relative to transgenics. Our engraftment rate is 84.4% overall and as high as 90%. A criticism of intravesical models is that the tumor may establish itself in off-target sites such as the ureter and kidney due to reflux or in the urethra due to pressure from bladder filling during inoculation. Our engraftment rates only include mice with tumors in the bladder that did not cause urinary tract obstruction. Off target engraftment in this model was $8.2 \pm 1.8\%$. This model is tightly confined to the target site as we did not observe tumors invading through the bladder wall or establishment of tumors outside the bladder.

In order to obtain our engraftment rate, we evaluated select previously utilized pre-treatment options. Various methods have been tested to increase cancer cell attachment by disrupting the glycosaminoglycan layer of the bladder or by separating or removing umbrella cells. We evaluated a pre-treatment of trypsin as used in a previous orthotopic xenograft [36] at a concentration of 0.25% for 15 minutes. Forty percent of mice showed gross hematuria and all xenografts grew slowly. We did not test physical bladder wall injury [21], or electrocautery [9, 17] as bladder damage has been found to cause undetected perforations and potential spread of the tumors to the intraperitoneal space [10]. Chemical damage using silver nitrate [20] and acid [43] was avoided due to expected hematuria in the nude mice as was found with trypsin treatment. We believe the cationic polypeptide, poly-L-lysine, for 15 minutes is the best alternative [16, 35, 40, 44]. Poly-L-lysine increases the electrostatic interaction between cells rather than damaging them and we have found no complications as yet from this pre-treatment. Furthermore, poly-L-lysine has been found to result in a smaller

percentage of invasive tumors in a rat model [45] although it did not increase engraftment over trypsin, acid or PBS. This may be because that model utilized a syngeneic, spontaneous tumor-derived cell line with different adherence properties than the human UM-UC-3 cells.

An important factor in establishing this model was the need for a superficial orthotopic xenograft bladder cancer model. An intramural orthotopic xenograft model that has been previously developed in our centre [19] and has been later adapted to a syngeneic model [11] is excellent for modelling muscle invasive bladder cancer but is not ideal for initially superficial tumors or intravesical therapy. The mentioned model involves tumor cell injection into the intramural space next to the muscle in the bladder wall. Both this model and our current model utilize bioluminescent imaging with ultrasound confirmation as had been previously validated [37]. Unfortunately, these tumors do not follow the natural history of originating in the epithelium and growing into the lumen prior to muscle invasion and as such cannot be used to model a superficial tumor. In addition, this model has an intact epithelium and any therapeutics that are delivered intravesically will first have to be evaluated for their ability to diffuse through the tightly sealed bladder wall. Our model allows for direct exposure to intravesical therapy similar to what occurs during BCG or chemotherapy following transurethral resection of bladder tumor (TURBT) in the clinical setting.

We believe that our model supplements the existing intramural model by providing a system to evaluate tumors prior to invasion, termed the superficial stage. Our cell line of choice, UM-UC-3-luc, developed reliable and reproducible tumors that are detectable within the first week post-implantation and represent a superficial phenotype as invasion was not observed in our model system. We believe that treatment of tumors in our model with experimental therapeutics recapitulates treatment of a superficial patient tumor to the closest extent that we can currently achieve.

Acknowledgements

Supported by the Canadian Institute of Health Research and TFRI NF PPG Project #1062.

Disclosure of conflict of interest

None.

Address correspondence to: Dr. Alan I So, Vancouver Prostate Centre, Department of Urologic Sciences, University of British Columbia, 2660 Oak Street, Vancouver, BC, V6H3Z6, Canada. E-mail: dralanso@mail.ubc.ca

References

- [1] Society CC. Canadian cancer statistics: a 2018 special report. 2018.
- [2] Schenk-Braat EA and Bangma CH. Immunotherapy for superficial bladder cancer. *Cancer Immunol Immunother* 2005; 54: 414-423.
- [3] Vargo-Gogola T and Rosen JM. Modelling breast cancer: one size does not fit all. *Nat Rev Cancer* 2007; 7: 659-672.
- [4] Armstrong E and Bonser G. Epithelial tumors of the urinary bladder in mice induced by 2-acetylaminofluorene. *Journal of Pathology* 1944; 6: 506-512.
- [5] Lijinsky W. Species differences in nitrosamine carcinogenesis. *J Cancer Res Clin Oncol* 1984; 108: 46-55.
- [6] Steinberg GD, Brendler CB, Ichikawa T, Squire RA and Isaacs JT. Characterization of an N-methyl-N-nitrosourea-induced autochthonous rat bladder cancer model. *Cancer Res* 1990; 50: 6668-6674.
- [7] Chala B, Choi MH, Moon KC, Kim HS, Kwak C and Hong ST. Development of urinary bladder pre-neoplasia by schistosoma haematobium eggs and chemical carcinogen in mice. *Korean J Parasitol* 2017; 55: 21-29.
- [8] Chan E, Patel A, Heston W and Larchian W. Mouse orthotopic models for bladder cancer research. *BJU Int* 2009; 104: 1286-1291.
- [9] Dobek GL and Godbey WT. An orthotopic model of murine bladder cancer. *J Vis Exp* 2011.
- [10] Horiguchi Y, Larchian WA, Kaplinsky R, Fair WR and Heston WD. Intravesical liposome-mediated interleukin-2 gene therapy in orthotopic murine bladder cancer model. *Gene Ther* 2000; 7: 844-851.
- [11] Lin T, Yuan A, Zhao X, Lian H, Zhuang J, Chen W, Zhang Q, Liu G, Zhang S, Chen W, Cao W, Zhang C, Wu J, Hu Y and Guo H. Self-assembled tumor-targeting hyaluronic acid nanoparticles for photothermal ablation in orthotopic bladder cancer. *Acta Biomater* 2017; 53: 427-438.
- [12] Nakamura T, Fukiage M, Suzuki Y, Yano I, Miyazaki J, Nishiyama H, Akaza H and Hara-shima H. Mechanism responsible for the anti-tumor effect of BCG-CWS using the LEEL method in a mouse bladder cancer model. *J Control Release* 2014; 196: 161-167.
- [13] Qiu X, Cao K, Lin T, Chen W, Yuan A, Wu J, Hu Y and Guo H. Drug delivery system based on dendritic nanoparticles for enhancement of intravesical instillation. *Int J Nanomedicine* 2017; 12: 7365-7374.
- [14] Roughan JV, Coulter CA, Flecknell PA, Thomas HD and Sufka KJ. The conditioned place preference test for assessing welfare consequences and potential refinements in a mouse bladder cancer model. *PLoS One* 2014; 9: e103362.
- [15] Seo HK, Shin SP, Jung NR, Kwon WA, Jeong KC and Lee SJ. The establishment of a growth-controllable orthotopic bladder cancer model through the down-regulation of c-myc expression. *Oncotarget* 2016; 8: 50500-50509.
- [16] Virani NA, Davis C, McKernan P, Hauser P, Hurst RE, Slaton J, Silvy RP, Resasco DE and Harrison RG. Phosphatidylserine targeted single-walled carbon nanotubes for photothermal ablation of bladder cancer. *Nanotechnology* 2018; 29: 035101.
- [17] Fazel J, Rotzer S, Seidl C, Feuerecker B, Autenrieth M, Weirich G, Bruchertseifer F, Morgens-tern A and Senekowitsch-Schmidtke R. Fractionated intravesical radioimmunotherapy with (213)Bi-anti-EGFR-MAb is effective without toxic side-effects in a nude mouse model of advanced human bladder carcinoma. *Cancer Biol Ther* 2015; 16: 1526-1534.
- [18] Hadaschik BA, Black PC, Sea JC, Metwalli AR, Fazli L, Dinney CP, Gleave ME and So AI. A validated mouse model for orthotopic bladder cancer using transurethral tumour inoculation and bioluminescence imaging. *BJU Int* 2007; 100: 1377-1384.
- [19] Jager W, Moskalev I, Janssen C, Hayashi T, Gust KM, Awrey S and Black PC. Minimally invasive establishment of murine orthotopic bladder xenografts. *J Vis Exp* 2014; e51123.
- [20] Kang MR, Yang G, Charisse K, Epstein-Barash H, Manoharan M and Li LC. An orthotopic bladder tumor model and the evaluation of intravesical saRNA treatment. *J Vis Exp* 2012.
- [21] Yang XH, Ren LS, Wang GP, Zhao LL, Zhang H, Mi ZG and Bai X. A new method of establishing orthotopic bladder transplantable tumor in mice. *Cancer Biol Med* 2012; 9: 261-265.
- [22] Cui M, Au JL, Wientjes MG, O'Donnell MA, Loughlin KR and Lu Z. Intravenous siRNA silencing of survivin enhances activity of mitomycin C in human bladder RT4 Xenografts. *J Urol* 2015; 194: 230-237.
- [23] Cui X, Shen D, Kong C, Zhang Z, Zeng Y, Lin X and Liu X. NF-kappaB suppresses apoptosis and promotes bladder cancer cell proliferation by upregulating survivin expression in vitro and in vivo. *Sci Rep* 2017; 7: 40723.
- [24] Gong Z, Xu H, Su Y, Wu W, Hao L and Han C. Establishment of a novel bladder cancer xenograft model in humanized immunodeficient mice. *Cell Physiol Biochem* 2015; 37: 1355-1368.

Murine model for bladder cancer

- [25] John BA, Xu T, Ripp S and Wang HR. A real-time non-invasive auto-bioluminescent urinary bladder cancer xenograft model. *Mol Imaging Biol* 2017; 19: 10-14.
- [26] Liu Z, Yokoyama NN, Blair CA, Li X, Avizonis D, Wu XR, Uchio E, Youssef R, McClelland M, Polak M and Zi X. High sensitivity of an Ha-RAS transgenic model of superficial bladder cancer to metformin is associated with approximately 240-fold higher drug concentration in urine than serum. *Mol Cancer Ther* 2016; 15: 430-438.
- [27] Wan W, Peng K, Li M, Qin L, Tong Z, Yan J, Shen B and Yu C. Histone demethylase JMJD1A promotes urinary bladder cancer progression by enhancing glycolysis through coactivation of hypoxia inducible factor 1 α . *Oncogene* 2017; 6: 3868-3877.
- [28] Yang R, Liu M, Liang H, Guo S, Guo X, Yuan M, Lian H, Yan X, Zhang S, Chen X, Fang F, Guo H and Zhang C. miR-138-5p contributes to cell proliferation and invasion by targeting Survivin in bladder cancer cells. *Mol Cancer* 2016; 15: 82.
- [29] Arantes-Rodrigues R, Colaco A, Pinto-Leite R and Oliveira PA. In vitro and in vivo experimental models as tools to investigate the efficacy of antineoplastic drugs on urinary bladder cancer. *Anticancer Res* 2013; 33: 1273-1296.
- [30] Madka V, Mohammed A, Li Q, Zhang Y, Kumar G, Lightfoot S, Wu X, Steele V, Kopelovich L and Rao CV. TP53 modulating agent, CP-31398 enhances antitumor effects of ODC inhibitor in mouse model of urinary bladder transitional cell carcinoma. *Am J Cancer Res* 2015; 5: 3030-3041.
- [31] Santos M, Martinez-Fernandez M, Duenas M, Garcia-Escudero R, Alfaya B, Villacampa F, Saiz-Ladera C, Costa C, Oteo M, Duarte J, Martinez V, Gomez-Rodriguez MJ, Martin ML, Fernandez M, Viatour P, Morcillo MA, Sage J, Castellano D, Rodriguez-Peralto JL, de la Rosa F and Paramio JM. In vivo disruption of an Rb-E2F-Ezh2 signaling loop causes bladder cancer. *Cancer Res* 2014; 74: 6565-6577.
- [32] Rosenberg MP and Bortner D. Why transgenic and knockout animal models should be used (for drug efficacy studies in cancer). *Cancer Metastasis Rev* 1998; 17: 295-299.
- [33] Thomas H and Balkwill F. Assessing new anti-tumour agents and strategies in oncogene transgenic mice. *Cancer Metastasis Rev* 1995; 14: 91-95.
- [34] Kubota T. Metastatic models of human cancer xenografted in the nude mouse: the importance of orthotopic transplantation. *J Cell Biochem* 1994; 56: 4-8.
- [35] Mangsbo SM, Ninalga C, Essand M, Loskog A and Totterman TH. CpG therapy is superior to BCG in an orthotopic bladder cancer model and generates CD4+ T-cell immunity. *J Immunother* 2008; 31: 34-42.
- [36] Watanabe T, Shinohara N, Sazawa A, Hara-bayashi T, Ogiso Y, Koyanagi T, Takiguchi M, Hashimoto A, Kuzumaki N, Yamashita M, Tanaka M, Grossman HB and Benedict WF. An improved intravesical model using human bladder cancer cell lines to optimize gene and other therapies. *Cancer Gene Ther* 2000; 7: 1575-1580.
- [37] Black PC, Shetty A, Brown GA, Esparza-Coss E, Metwalli AR, Agarwal PK, McConkey DJ, Hazle JD and Dinney CP. Validating bladder cancer xenograft bioluminescence with magnetic resonance imaging: the significance of hypoxia and necrosis. *BJU Int* 2010; 106: 1799-1804.
- [38] DeGraff DJ, Robinson VL, Shah JB, Brandt WD, Sonpavde G, Kang Y, Liebert M, Wu XR and Taylor JA 3rd. Current preclinical models for the advancement of translational bladder cancer research. *Mol Cancer Ther* 2013; 12: 121-130.
- [39] Saito B. [A study of BBN induced bladder cancer in mice. The time differences in changes of histopathology and nuclear DNA content]. *Nihon Hinyokika Gakkai Zasshi* 1991; 82: 1206-1210.
- [40] Chan ES, Patel AR, Smith AK, Klein JB, Thomas AA, Heston WD and Larchian WA. Optimizing orthotopic bladder tumor implantation in a syngeneic mouse model. *J Urol* 2009; 182: 2926-2931.
- [41] Jager W, Horiguchi Y, Shah J, Hayashi T, Awrey S, Gust KM, Hadaschik BA, Matsui Y, Anderson S, Bell RH, Ettinger S, So AI, Gleave ME, Lee IL, Dinney CP, Tachibana M, McConkey DJ and Black PC. Hiding in plain view: genetic profiling reveals decades old cross contamination of bladder cancer cell line KU7 with HeLa. *J Urol* 2013; 190: 1404-1409.
- [42] Roife D, Kang Y, Wang L, Fang B, Swisher SG, Gershenwald JE, Pretzsch S, Dinney CP, Katz MHG and Fleming JB. Generation of patient-derived xenografts from fine needle aspirates or core needle biopsy. *Surgery* 2017; 161: 1246-1254.
- [43] Yu DS, Lee CF and Chang SY. Immunotherapy for orthotopic murine bladder cancer using bacillus Calmette-Guerin recombinant protein Mpt-64. *J Urol* 2007; 177: 738-742.
- [44] Tham SM, Esuvaranathan K and Mahendran R. A murine orthotopic bladder tumor model and tumor detection system. *J Vis Exp* 2017.
- [45] Miyazaki K, Morimoto Y, Nishiyama N, Satoh H, Tanaka M, Shinomiya N and Ito K. Preconditioning methods influence tumor property in an orthotopic bladder urothelial carcinoma rat model. *Mol Clin Oncol* 2014; 2: 65-70.